Uniform and Sampled Bragg Gratings in SOI Strip Waveguides with Sidewall Corrugations

Xu Wang, *Student Member, IEEE,* Wei Shi, *Student Member, IEEE,* Raha Vafaei, Nicolas A. F. Jaeger, *Member, IEEE,* and Lukas Chrostowski, *Member, IEEE*

***Abstract*—We have demonstrated uniform and sampled Bragg gratings in silicon-on-insulator strip waveguides with symmetric sidewall corrugations. The fabrication is based on 193 nm deep ultra-violet lithography using a single mask. The measured reflection spectra of sampled gratings exhibit 10 usable peaks spaced by 4.2 nm, and show good agreement with theoretical predictions.**

***Index Terms*—Bragg gratings, sampled gratings, silicon-on-insulator, strip waveguides.**

I. Introduction

BRAGG grating structures are widely used in optical communication and sensing systems, such as in semiconductor lasers and fibers. Recently, the integration of Bragg gratings on the silicon-on-insulator (SOI) platform has been attracting much interest [1]. Several approaches have been reported to achieve periodic modulation of the effective index of refraction in SOI waveguides: (1) using photorefractive effects via selective ion implantation [2]; (2) physically corrugating the waveguide, either on the top surface [1] or on the sidewalls [3], [4]; and (3) placing periodic corrugations next to the waveguide [5], [6]. Although the first approach can retain a planar surface that may be useful for subsequent processing, the ion implantation makes the fabrication more expensive. Typically, electron-beam lithography (EBL) was the workhorse for the fabrication of SOI Bragg gratings, but is unsuitable for commercial applications [7]. An alternative is to use deep ultra-violet (DUV) lithography, with high throughput and low cost, which has been recently demonstrated in [8] and [9]: the gratings in [8] were top-surface corrugated, hence requiring double-exposure lithography and precise alignment, while the sidewall-corrugated configuration in [9] can be used to define the waveguide and gratings in a single lithography step, which is much simpler and less expensive.

Sampled gratings, an important derivative of Bragg gratings, are constructed by multiplying a sampling function and a conventional grating. Since the sampling function leads to a reflection spectrum with periodic maxima, sampled gratings are deployed in tunable semiconductor lasers to achieve wide tuning range through the Vernier effect [10].

Manuscript received October 22, 2010; revised December 14, 2010. This work was supported in part by the Natural Sciences and Engineering Research Council of Canada.

The authors are with the Department of Electrical and Computer Engineering, University of British Columbia, Vancouver, BC, V6T 1Z4, Canada (e-mail: xuw@ece.ubc.ca, lukasc@ece.ubc.ca)

Digital Object Identifier 00.0000/LPT.2010.0000000

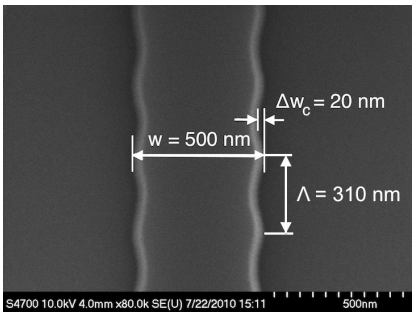

Fig. 1. Top view SEM image of a fabricated Bragg gratings. The designed square corrugation width is 25 nm with 50% duty cycle. The fabricated grating shape is rounded and the amplitude is reduced to ∼20 nm, due to the 193 nm lithography limitations.

In this letter, we present sidewall-corrugated Bragg gratings in compact SOI strip waveguides fabricated by 193 nm DUV lithography with a single mask. The fabricated corrugations are much smaller than in [9] allowing a narrow bandwidth of 0.8 nm to be achieved. Based on the sidewall-corrugated grating structure, we present the first demonstration of sampled gratings in silicon waveguides.

II. Uniform Gratings in SOI waveguides

Fig. 1 shows the scanning electron micrograph (SEM) of a fabricated Bragg grating, fabricated at IMEC ePIXfab [7] using 193 nm DUV lithography in a single step. The SOI strip waveguide consists of a thin silicon layer (220 nm thick) on top of a buried oxide layer (2 μm thick) on a silicon wafer. The strip width w is 500 nm, and the corrugations are recessed on both sidewalls. The corrugation width on each side Δw_c is approximately 20 nm in Fig. 1, which is much smaller than previous reports of similar gratings [3], [4], [9]. For all the devices reported here, the grating period Λ is 310 nm, the grating duty cycle is 50%, and the grating length L is 620 μm.

The chip layout schematic is shown in Fig. 2, where high-efficiency integrated grating couplers [7] were used as input and output ports and AR coated lensed polarization-maintaining fibers were used for efficient vertical fiber coupling. The grating couplers were designed for transverse electric (TE) polarization only. A Y-branch splitter was used to collect the reflected light. The grating transmission was normalized using the transmission of a simple waveguide. The grating reflection was similarly normalized with the additional 3 dB Y-branch splitter loss. Therefore, in both cases, the losses due to propagation and fiber coupling have been de-embedded.

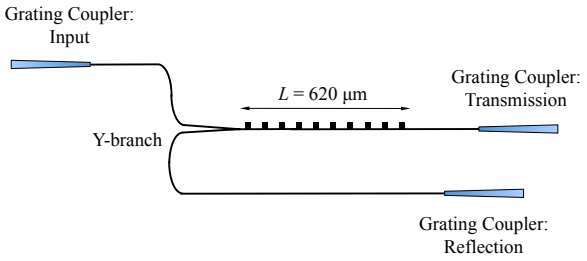

Fig. 2. Schematic of the chip layout designed to measure the reflection and transmission spectrum of TE-mode uniform and sampled Bragg gratings. Normalization was performed using a straight-through waveguide (not shown). The spectra were measured using an HP 81682A tunable laser and detector.

The measured reflection and transmission spectra are shown in Fig. 3. As can be seen in Fig. 3(b), the loss introduced by the gratings is negligible. As the corrugation width is increased, the average effective index of refraction n_{eff} decreases [6], hence shifting the reflectivity peak to shorter wavelength by the Bragg condition, $\lambda_0 = 2n_{eff}\Lambda$, where λ_0 is the Bragg wavelength. To keep λ_0 roughly constant, symmetric corrugations (relative to the edge of the straight waveguide) can be used. Since all devices have the same length, the peak reflectivity and the bandwidth is determined only by the coupling coefficient κ [10]:

$$R_{peak} = \tanh^2(\kappa L), \quad \Delta\lambda_{1/2} = \frac{\lambda_0^2}{\pi n_g}\sqrt{\kappa^2 + (\pi/L)^2} \quad (1)$$

where n_g is the group index. As the corrugation width is increased, the coupling coefficient increases, leading to higher reflectivity and broader bandwidth, as shown in Fig. 3.

It should be noted that square modulation was used in our mask design and the corrugation is smaller than the lithography resolution (∼90 nm); thus the gratings actually fabricated are severely rounded and the amplitudes are reduced, as can be seen in Fig. 1. To simulate the effect of fabrication [9], we present the measured bandwidth versus the designed corrugation width, compared with the simulation results using different shapes, in Fig. 4. The simulation was done using a 2D mode solver [11]. The results show that for a designed 20 nm square corrugation, the measured bandwidth is significantly lower than in the simulations and is approximately equal to the simulated bandwidth of a 5 nm square corrugation, i.e., its "effective" square-corrugation is only 5 nm. This fact may be useful in future designs to approximately adjust the mask layout to compensate for the lithographic limitations. The simulated transmission spectrum using this effective corrugation also agrees with the measured response, as shown in Fig. 3(b). The minimum measured bandwidth is 0.8 nm (for a designed corrugations of 10 nm); it is possible to achieve narrower bandwidth by moving the corrugations outside the waveguide itself [6], and which allows precise control of the coupling coefficient and overcomes the lithography limitations.

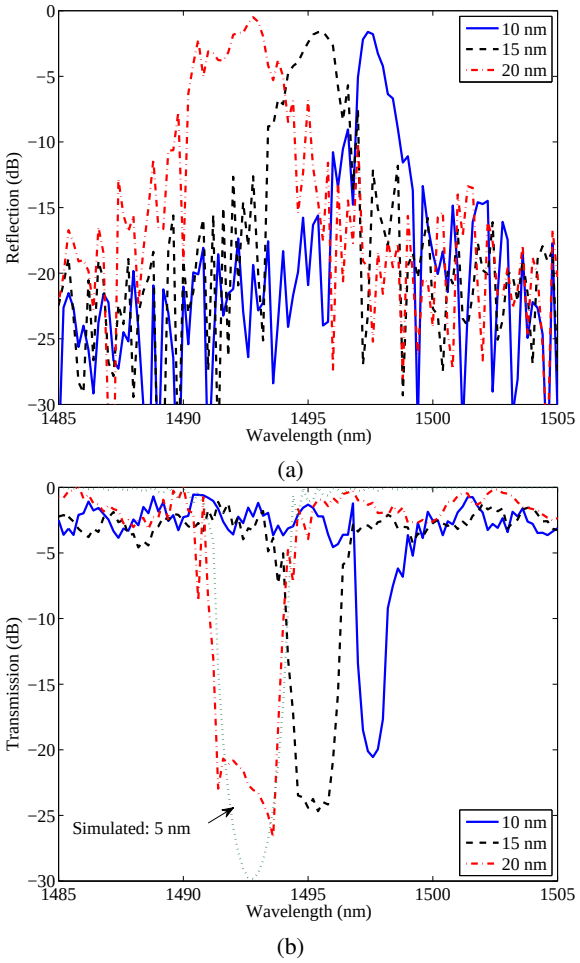

Fig. 3. Measured reflection and transmission spectra of designed uniform gratings for varied corrugation width. The simulated transmission spectrum in (b) is for 5 nm square corrugation, which agrees with the measured response of the device with 20 nm square corrugation in design.

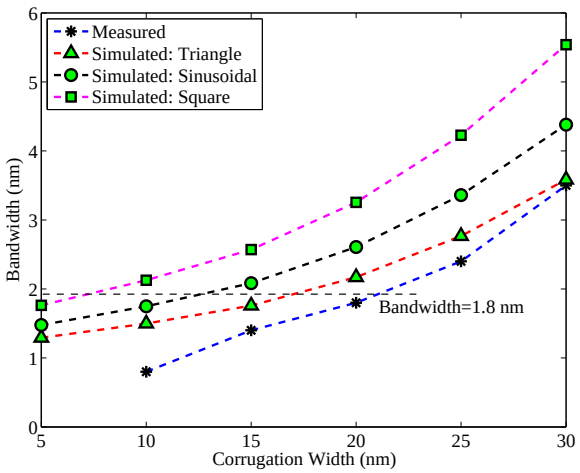

Fig. 4. Measured and simulated bandwidth versus designed corrugation width. To achieve a bandwidth of 1.8 nm, the corrugation width should be 5 nm, 10 nm, and 15 nm for square, sinusoidal, and triangle corrugations in simulation, and 20 nm in the mask designed for fabrication, respectively.

III. Sampled Gratings in SOI Waveguides

Fig. 5 illustrates the proposed sampled grating structure. The grating burst length Z_1 is 6.2 μm (20 grating periods), and the burst period Z_0 is 62 μm, therefore, the duty cycle of the sampling function is $Z_1/Z_0 = 0.1$. The total length L is still 620 μm, including ten sampling periods.

The measured reflection spectra are shown in Fig. 6, where

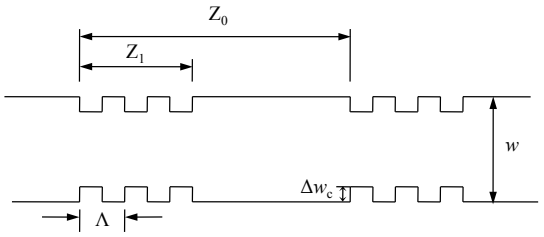

Fig. 5. Sampled grating structure.

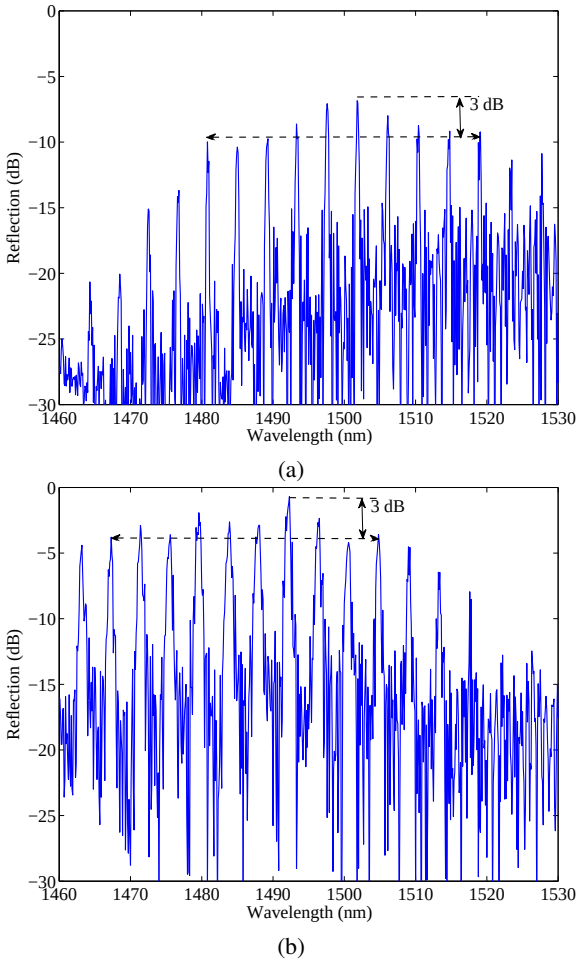

Fig. 6. Measured reflection spectra of sampled gratings: (a) designed corrugation width is 20 nm, and (b) designed corrugation width is 40 nm.

periodic maxima were clearly observed and centred at the Bragg wavelength, as predicted in [10]. Since increasing the corrugation width reduces the Bragg wavelength, the envelope of the reflectivity peaks is shifted to the left, as shown in Fig. 6. The spacing between reflectivity peaks is given by [10], $\Delta\lambda = \lambda^2/2n_g Z_0$. The measured spacing is about 4.2 nm, showing a group index of about 4.32, which is in good agreement with the calculations using the mode solver [11]. In Fig. 6, the number of peaks in the 3 dB envelope of the reflection spectra is 10, which agrees with the theoretical prediction [10], $N_{3db} \approx Z_0/Z_1$.

In Section II, we have shown that the peak reflectivity and bandwidth of uniform gratings is determined by the coupling coefficient. Similarly, for sampled gratings, each reflectivity peak has a corresponding coupling coefficient, which is proportional to the unsampled one [10]. Therefore, as the corrugation width is increased, the coupling coefficients become larger, resulting in higher reflectivity and broader bandwidth for all peaks, which can also be observed in Fig. 6.

IV. Conclusion

We have demonstrated Bragg gratings in SOI strip waveguides fabricated by a single DUV lithography step. A bandwidth of 0.8 nm was achieved for our 10 nm (as designed) sidewall corrugations. We also demonstrated sampled gratings, and the measured reflection spectra show 10 usable peaks over a wavelength range of more than 40 nm. As compared to ring resonators, there is more design freedom in sampled gratings which allows a further degree of control on the spectrum, e.g., enhanced extinction ratios. The comb-like reflection spectrum, combined with the potential for using the Vernier effect, makes this device interesting for future applications in silicon-based integrated systems, such as in tunable silicon lasers, multichannel add/drop multiplexers, and biosensors.

Acknowledgment

The authors would like to thank CMC Microsystems for making this project possible, Lumerical Solutions Inc. and Design Workshop Technologies for the design tools.

References

[1] T. E. Murphy, J. T. Hastings, and H. I. Smith, "Fabrication and characterization of narrow-band Bragg-reflection filters in silicon-on-insulator ridge waveguides," *J. Lightwave Technol.*, vol. 19, no. 12, pp. 1938–1942, 2001.

[2] S. Homampour, M. P. Bulk, P. E. Jessop, and A. P. Knights, "Thermal tuning of planar Bragg gratings in silicon-on-insulator rib waveguides," *Phys. Status Solidi C*, no. S1, pp. S240–S243, 2009.

[3] J. T. Hastings, M. H. Lim, J. G. Goodberlet, and H. I. Smith, "Optical waveguides with apodized sidewall gratings via spatial-phase-locked electron-beam lithography," *J. Vac. Sci. Technol. B*, vol. 20, no. 6, pp. 2753–2757, 2002.

[4] A. S. Jugessur, J. Dou, J. S. Aitchison, R. M. De La Rue, and M. Gnan, "A photonic nano-Bragg grating device integrated with microfluidic channels for bio-sensing applications," *Microelectronic Engineering*, vol. 86, no. 4-6, pp. 1488–1490, 2009.

[5] D. T. H. Tan, K. Ikeda, and Y. Fainman, "Cladding-modulated Bragg gratings in silicon waveguides," *Opt. Lett.*, vol. 34, no. 9, pp. 1357–1359, 2009.

[6] X. Wang, W. Shi, R. Vafaei, N. A. F. Jaeger, and L. Chrostowski, "Silicon-on-insulator Bragg gratings fabricated by deep UV lithography," in *IEEE Asia Communications and Photonics Conf.*, 12/2010 2010.

[7] W. Bogaerts, R. Baets, P. Dumon, V. Wiaux, S. Beckx, D. Taillaert, B. Luyssaert, J. V. Campenhout, P. Bienstman, and D. V. Thourhout, "Nanophotonic waveguides in silicon-on-insulator fabricated with CMOS technology," *J. Lightwave Technol.*, vol. 23, no. 1, pp. 401–412, 2005.

[8] I. Giuntoni, D. Stolarek, H. Richter, S. Marschmeyer, J. Bauer, A. Gajda, J. Bruns, B. Tillack, K. Petermann, and L. Zimmermann, "Deep-UV technology for the fabrication of Bragg gratings on SOI rib waveguides," *IEEE Photon. Technol. Lett.*, vol. 21, no. 24, pp. 1894–1896, 2009.

[9] W. Bogaerts, P. Bradt, L. Vanholme, P. Bienstman, and R. Baets, "Closed-loop modeling of silicon nanophotonics from design to fabrication and back again," *Opt. Quant. Electron.*, vol. 40, no. 11-12, pp. 801–811, 2008.

[10] V. Jayaraman, Z.-M. Chuang, and L. A. Coldren, "Theory, design, and performance of extended tuning range semiconductor lasers with sampled gratings," *IEEE J. Quantum Electron.*, vol. 29, no. 6, pp. 1824–1834, 1993.

[11] *Software:* MODE Solutions, Lumerical Solutions, Inc.